Relative Distance Control of Uncooperative Tethered Debris

Liam Field, Eleonora M. Botta

Department of Mechanical & Aerospace Engineering
University at Buffalo, SUNY

January 16, 2023

Outline

Outline

1. Introduction
2. System Modeling and Control
3. Simulation Results
4. Sensitivity Study
5. Conclusion
6. Estimation and Control

Tether-Based Active Debris Removal

Active debris removal by means of interconnection through a flexible tether is a promising option. The primary means of capture through such a tether are:

- Nets
- Harpoons

The flexible connection introduces **complex dynamics in the post-capture phases** of the ADR mission that the chaser craft must manage, particularly the slackness in the tether.

Relative distance controllers have been proposed (Jaworski et al., 2017; Cleary and O'Connor, 2016).

Objectives:

- Propose PD and PID controllers
- Investigate dynamics of the tethered system

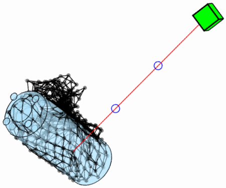

Outline

Model Assumptions and Layout

- Assumptions
  1. Rigid chaser (cube) and target (rectangular prism)
  2. No external forces other than gravity and tether tension
  3. Kelvin-Voigt tether model
- Important frame definitions
  - $\mathcal{O} = [\hat{\boldsymbol{I}}, \hat{\boldsymbol{J}}, \hat{\boldsymbol{K}}]$
  - $\mathcal{C} = [\hat{\boldsymbol{c}}_1, \hat{\boldsymbol{c}}_2, \hat{\boldsymbol{c}}_3]$
  - $\mathcal{T} = [\hat{\boldsymbol{t}}_1, \hat{\boldsymbol{t}}_2, \hat{\boldsymbol{t}}_3]$

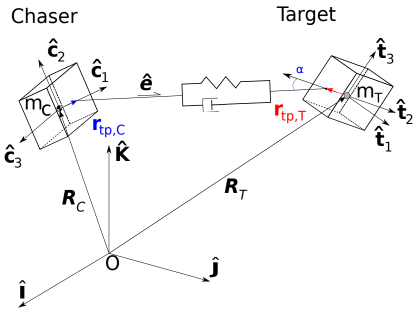

$\alpha =$ alignment angle

Kinematics and Dynamics

Translational dynamics: $m\ddot{\boldsymbol{R}} = -m\mu\dfrac{\boldsymbol{R}}{||\boldsymbol{R}||^3} + \boldsymbol{T} + \boldsymbol{U}$

$$\boldsymbol{T} \rightarrow \text{Tension } \boldsymbol{U} \rightarrow \text{Control Input}$$

Target attitude: represented by a unit quaternion $\boldsymbol{q} = [q_0, \boldsymbol{q}_v]^T$, with $\boldsymbol{q}_v = [q_1, q_2, q_3]$.

Kinematic relationship between the attitude and angular rates:

$$\dot{\boldsymbol{q}} = \frac{1}{2}\begin{bmatrix} -q_1 & -q_2 & -q_3 \\ q_0 & -q_3 & q_2 \\ q_3 & q_0 & -q_1 \\ -q_2 & q_1 & q_0 \end{bmatrix}\begin{bmatrix} \omega_x \\ \omega_y \\ \omega_z \end{bmatrix}$$

Rotational dynamics for body X:

$$\dot{\boldsymbol{\omega}} = J_X^{-1}({}^{\mathcal{X}}\boldsymbol{r}_{tp,X} \times {}^{\mathcal{X}}A^{\mathcal{O}}\boldsymbol{T} - \boldsymbol{\omega} \times J_X\boldsymbol{\omega} + \boldsymbol{\tau})$$

where $\mathcal{X}$ is its respective body fixed frame (e.g. ${}^{\mathcal{C}}\boldsymbol{r}_{tp,C}$).

Tether Modeling

- Cannot support compression
- No twisting or bending modeled

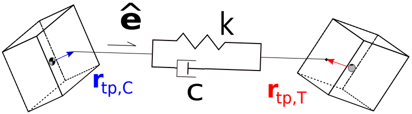

Tether Tension Vector: $\boldsymbol{T} = \begin{cases} T\hat{\mathbf{e}} & \text{if} \quad (l > l_0) \wedge (T > 0), \\ 0 & \text{if} \quad (l \leq l_0) \vee (T \leq 0). \end{cases} \quad T = k(l - l_0) + c\dot{l}$

$$k = \text{stiffness} \;\; c = \text{damping} \;\; l_0 = \text{natural length} \;\; \delta l = \text{elongation}$$

Tether Heading Vector: $\hat{\mathbf{e}} = \dfrac{\boldsymbol{R}_T +^{\mathcal{O}} \boldsymbol{r}_{tp,T} - \boldsymbol{R}_C -^{\mathcal{O}} \boldsymbol{r}_{tp,C}}{||\boldsymbol{R}_T +^{\mathcal{O}} \boldsymbol{r}_{tp,T} - \boldsymbol{R}_C -^{\mathcal{O}} \boldsymbol{r}_{tp,C}||}$

Tether Length and Length Rate: $l = ||\boldsymbol{R}_T +^{\mathcal{O}} \boldsymbol{r}_{tp,T} - \boldsymbol{R}_C -^{\mathcal{O}} \boldsymbol{r}_{tp,C}||$

$$\dot{l} = (\boldsymbol{V}_T +^{\mathcal{O}} \boldsymbol{A}^{\mathcal{T}} \boldsymbol{\omega}_T \times^{\mathcal{T}} \boldsymbol{r}_{tp,T} - \boldsymbol{V}_C -^{\mathcal{O}} \boldsymbol{A}^{\mathcal{C}} \boldsymbol{\omega}_C \times^{\mathcal{C}} \boldsymbol{r}_{tp,C}) \cdot \hat{\mathbf{e}}$$

Relative Distance Control

Process Variable: $e = \Delta l + l_0 - l$

$$\Delta l = \text{desired elongation}$$

PID/PD Input Thrust Magnitudes:

- $F_{PID} = K_P e + K_I \int_0^t e\,dt + K_D \dot{e}$
- $F_{PD} = K_p e + K_d \dot{e}$

PID/PD Input Thrust Directions:

- $\boldsymbol{F}_{PID} = -F_{PID}\hat{\boldsymbol{e}}$
- $\boldsymbol{F}_{PD} = -F_{PD}\hat{\boldsymbol{e}}$

For comparison, open loop control:

$$\boldsymbol{F}_{OL} = -20\hat{\boldsymbol{V}}_C$$

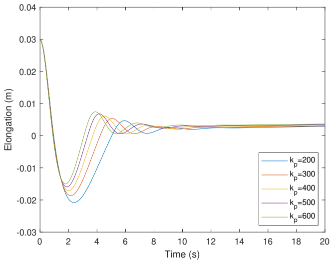

Heuristic tuning of gains, with desired elongation of 0.01 m.

Chaser Attitude Control

Desired chaser axes:

$$^{\mathcal{O}}A_d^{\mathcal{C}} = [\hat{\boldsymbol{e}} \mid (\hat{\boldsymbol{e}} \times \hat{\boldsymbol{R}}_C) \times \hat{\boldsymbol{e}} \mid \hat{\boldsymbol{e}} \times \hat{\boldsymbol{R}}_C]$$

Outline

Simulations for Controller Performance Analysis

Two scenarios:

- Initially taut tether: $\delta l = 3 \times 10^{-5}$ m
- Initially slack tether: $\delta l = -1$ m

Initial $\alpha = \pi/6$ rad: imperfect capture scenario.
Scenarios simulated for 500 s.

$K_P = 300$ N/m $\quad K_D = 2000$ Ns/m
$K_I = 300$ N/ms

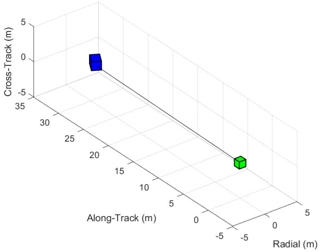

System parameters for the simulation scenarios.

Parameter	Value	Parameter	Value
J_C (kg-m^2)	diag(83.3, 83.3, 83.3)	m_C (kg)	500
J_T (kg-m^2)	diag(15000, 3000, 15000)	m_T (kg)	3000
${}^{\mathcal{C}}\boldsymbol{r}_{tp,C}$ (m)	$[0.5, 0, 0]^T$	k (N/m)	1573
${}^{\mathcal{T}}\boldsymbol{r}_{tp,T}$ (m)	$[0, -0.875, 0]^T$	c (Ns/m)	16
l_0 (m)	30	$\boldsymbol{\omega}_T$ (rad/s)	$[0, 0.05, 0]^T$

Initially Taut Tether

- PID control achieves δl of 0.01 m
- PD control steady state δl at $\sim$ 0.0014 m.

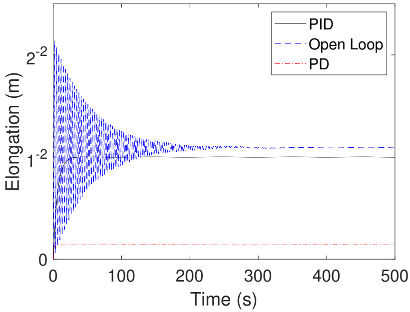

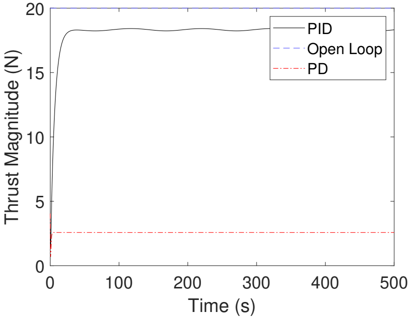

Initially Taut Tether - Continued

- Lower applied moment from PD control.
- Open loop α behavior result of its thrust direction.

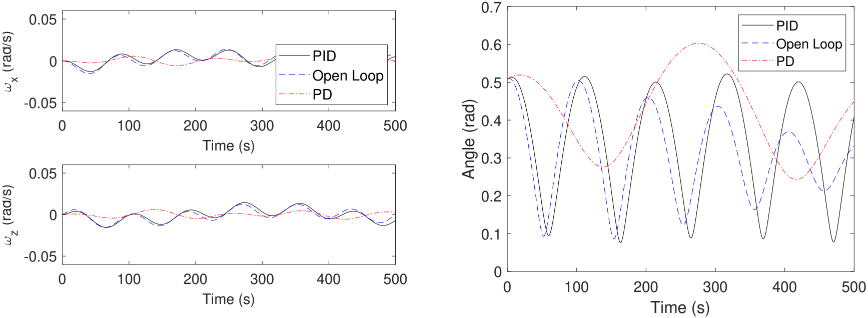

Initially Slack Tether

- PID control results in 0.25m peak δl
- PD control steady state δl again ~ 0.0014 m

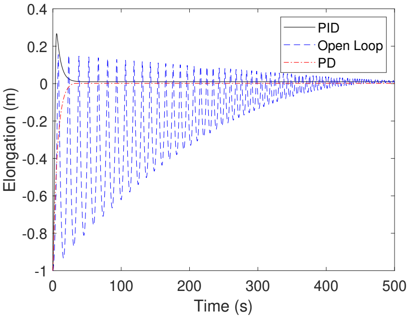

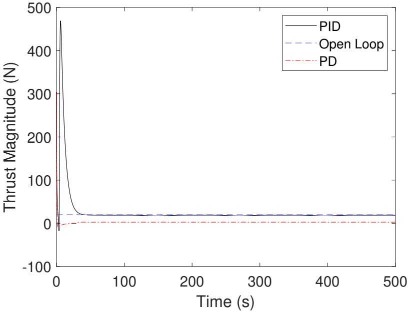

Initially Slack Tether - Continued

- Relaxation of tether tension in PID control causes large α.
- PD and open loop result in similar $\boldsymbol{\omega}$ and α as the previous scenario.

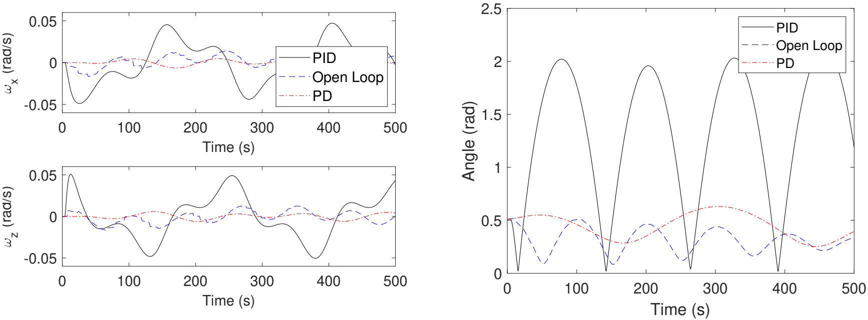

Initially Slack Tether - Continued

- PD α difference caused by time when $T > 0$.
- For PID, K_I responsible for large peak δl.
- For PID, steady-state applied moment insufficient to counter initial angular impulse.

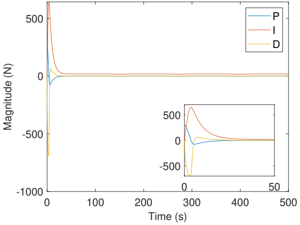

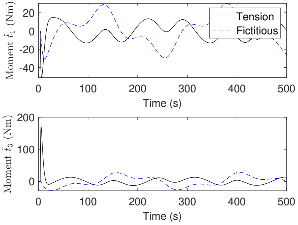

Discussion

- PID controller introduces dangerous motion of the debris; T larger than w/ PD control.
- PD control does not achieve desired Δl; similar behavior in both simulations.

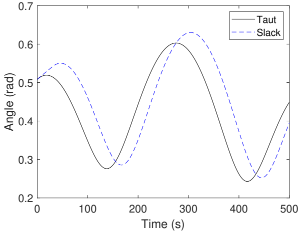

Outline

Sensitivity Study Setup

System parameters (target's especially) are uncertain. Sensitivity study conducted on **key variables**:

- Target Mass
- Target Moments of Inertia
- Initial Angular Rates
- Initial Relative Distance

Outputs to analyze the variations in the dynamics:

- Peak alignment angle α_{max}
- Control effort E_c
- Integrated squared norm of the angular rates W

$$W = \int_0^t ||\boldsymbol{\omega}||^2 dt \qquad E_c = \int_0^t |F_{PD}| dt$$

Variable	Error Bound
Target Mass	$\pm$300 kg
Target Inertia Matrix	$\pm$ diag[3000 600 3000] kg-m^2
Target Angular Rates	$\pm$0.04 rad/s
Initial Rel. Distance	$\pm$0.3 m

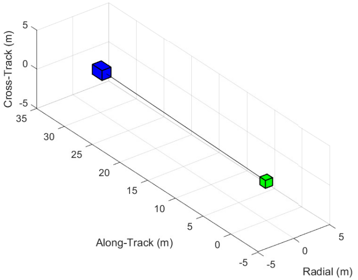

Target Mass Study

- Decreased mass → more responsive target.
- Angular rate integral W increases with mass.
- Differences marginal.

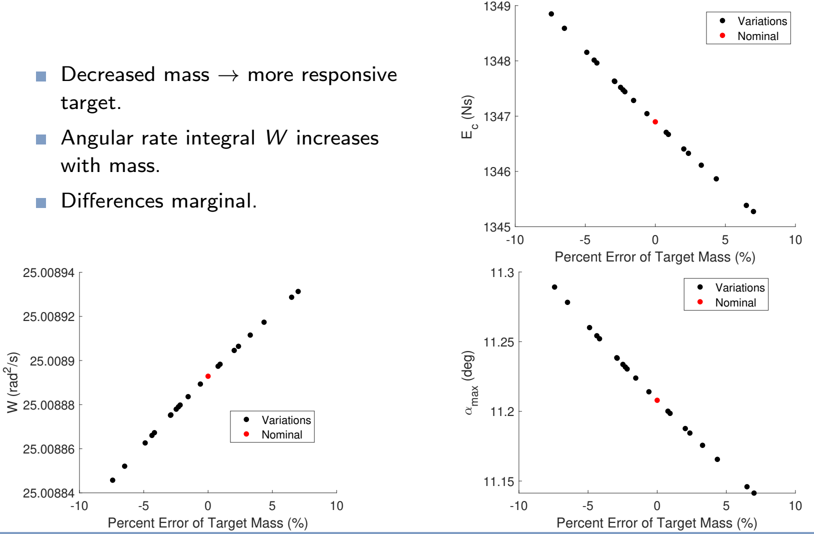

Target Moments of Inertia Study

- Asymmetry in J_x and J_z $\rightarrow$ non-zero $\dot{\omega}_y$.
- More significant variations in α_{max} and W.
- E_c differences order of 10^{-3} Ns.
- Varying J_y has the largest impact on α_{max}.

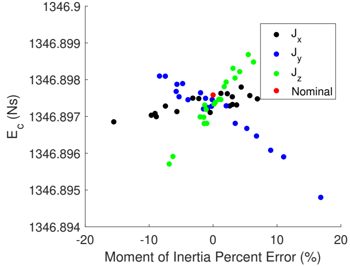

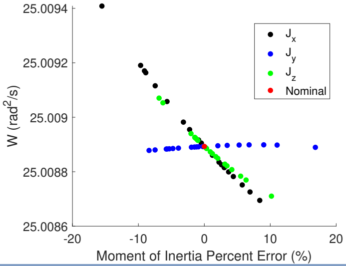

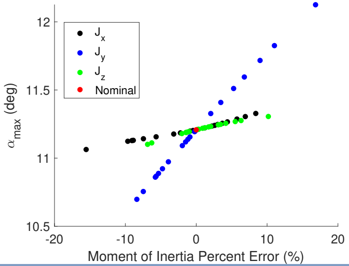

Target Angular Rates Study

- Quadratic trends in ω_x and ω_z.
- Tumbling motion exceeds ability of PD controller.
- Inertial velocity of target attachment point increased.

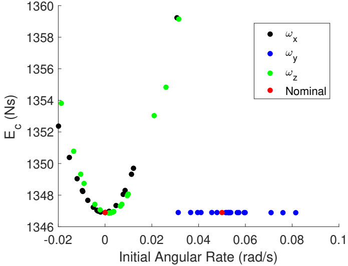

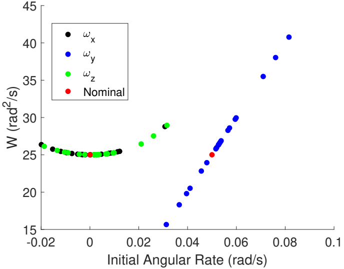

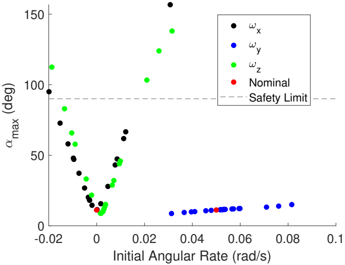

Initial Relative Distance Study

- E_c increases as chaser gets closer.
- Effects on α_{max} and W caused by chaser's motion when $T < 0$.
- PD control capable of handling this uncertainty.

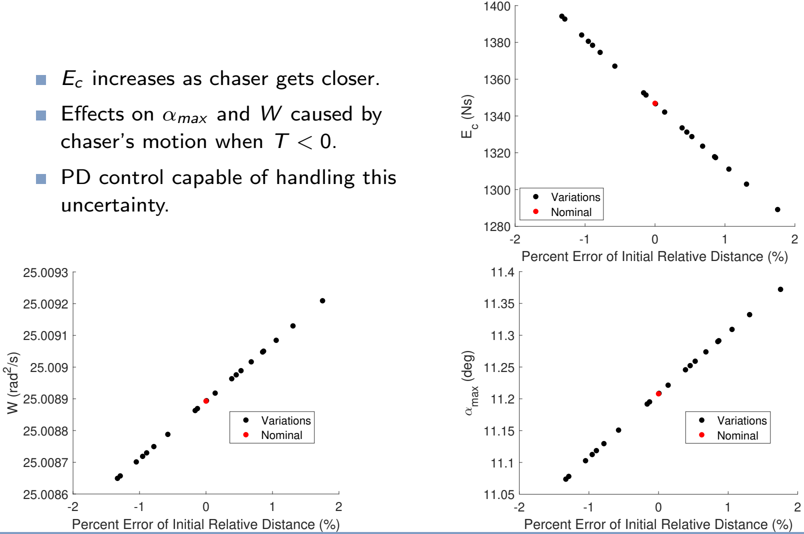

Outline

Conclusion

Proposed PD and PID controllers to maintain a relative distance between the chaser and target.

- **PID control:**
  - Possible tether winding $\rightarrow$ Unsuited for this purpose.
- **PD control:**
  - Induced more relaxed angular motion on the target.
  - Capable of handling uncertainty in target inertia properties and initial relative distance.
  - Cannot maintain safe target attitude motion in certain circumstances.

Future Work

- Apply PD control alongside target state estimation.
- Active target attitude control.

Outline

Online Estimation and Control

- Currently assuming image processing and subsequent update is achieved instantaneously at t_k (i.e., at t_k, $\boldsymbol{X}_k^-$ is updated to $\boldsymbol{X}_k^+$ which is used for control calculation).
- Measurement frequency of 10 Hz. and tracking 5 feature points.
- Using PID control with saturation at 50 N to get best estimates at the moment.

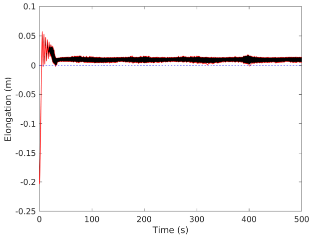

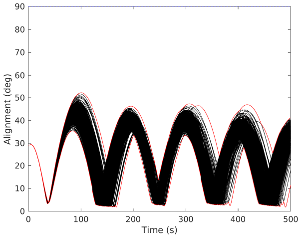

Online Estimation and Control

- The final estimate distributions for J_x, J_y, and J_z are within 3.62%, 0.541%, and 3.81% of the true values, respectively.

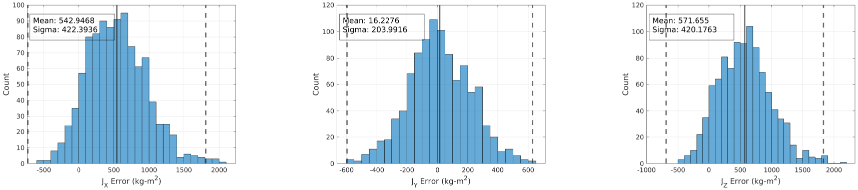

Thank you for your time.

Questions?

liamfiel@buffalo.edu
ebotta@buffalo.edu

Acknowledgements: Funded by the National Science Foundation Award# CRII: RI:2105011